

# 10K Ring Electrode Trap - Tandem Mass Spectrometer for Infrared Spectroscopy of Mass Selected Ions

Daniel J. Goebbert<sup>a,b</sup>, Gerard Meijer<sup>a</sup> and Knut R. Asmis<sup>a</sup>

<sup>a</sup> *Fritz-Haber-Institut der Max-Planck-Gesellschaft, Faradayweg 4-6, 14195 Berlin, Germany.*

<sup>b</sup> *Present address: Department of Chemistry, University of Arizona, Tucson, Arizona 85721-0041.*

**Abstract.** A novel instrumental setup for measuring infrared photodissociation spectra of buffer gas cooled, mass-selected ions is described and tested. It combines a cryogenically cooled, linear radio frequency ion trap with a tandem mass spectrometer, optimally coupling continuous ion sources to pulsed laser experiments. The use of six independently adjustable DC potentials superimposed over the trapping radio frequency field provides control over the ion distribution within, as well as the kinetic energy distribution of the ions extracted from the ion trap. The scheme allows focusing the ions in space and time, such that they can be optimally irradiated by a pulsed, widely tunable infrared photodissociation laser. Ion intensities are monitored with a time-of-flight mass spectrometer mounted orthogonally to the ion trap axis.

**Keywords:** Ring electrode ion trap, infrared photodissociation spectroscopy, mass-selected ions.

**PACS:** 07.75.+h, 33.20.Ea, 37.10.Ty, 82.80.Gk.

## INTRODUCTION

The structural characterization of larger gas phase ions constitutes a very challenging and active research area. Standard characterization techniques known from condensed phase, like absorption, NMR and X-ray diffraction spectroscopy, are not easily applicable in the gas phase, mainly due to space charge effects resulting in too low number densities ( $\sim <10^8$  ions/cm<sup>3</sup>). Therefore a variety of indirect techniques have been developed, from which the structure of the ion is deduced. While reactivity and collision induced dissociation experiments are often not specific enough, trapped ion diffraction<sup>1,2</sup>, ion mobility measurements<sup>3,4</sup> and vibrational spectroscopy<sup>5,6</sup> are promising approaches. In particular, infrared photodissociation (IRPD) spectroscopy paired with quantum chemistry<sup>7,8</sup> may currently offer the most direct and generally applicable experimental approach to structural investigation of molecular and cluster ions in the gas phase.

Here, we report our recent development of a novel instrument for the purpose of measuring IRPD spectra of mass-selected and buffer gas cooled ions. In the development of this instrument we sought to fulfill a number of goals. First, a wide variety of pulsed as well as continuous ion sources should be mountable, requiring that the ion production process is decoupled from the pulsed laser irradiation step. Second,

ions should be buffer gas cooled down to cryogenic temperatures to ensure that the lowest energy isomer in its vibrational ground state is exclusively populated. Third, the ion detection efficiency should be optimized.

The first goal is achieved by employing an ion trap, which allows storing ions and extracting them on demand. This decouples the ion production rate from the repetition rate of the laser experiment. Linear multipole radio frequency (RF) ion traps have been used to great effect in this regard.<sup>9,10</sup> The second goal is met by employing a cryogenically cooled, gas-filled ion trap.<sup>11-13</sup> Multiple collisions with cold He atoms will thermalize the ions close to the trap temperature. For multipole RF ion traps, ion temperatures below 10 K have been reported, sufficient to obtain vibrationally cold ions.<sup>14,15</sup> However, these traps are usually used in combination with quadrupole mass filters, which allow to monitor the intensity of only a single ion at a time. Coupling a linear RF ion trap to a time-of-flight (TOF) mass spectrometer is more efficient in that it allows to monitor all fragment ion intensities simultaneously, but this adds some additional complexity to the experiment.<sup>16</sup> The ions occupy a large spatial volume in the linear ion trap, while a TOF sampling aperture has a limited spatial extent. In order to achieve high collection efficiencies at the TOF detector the diffuse ion cloud from the trap must be spatially and temporally focused. This is ideally done using a ring-electrode-trap as originally shown by Gerlich and coworkers.<sup>16</sup> The ring-electrode-trap allows tailoring the electric field along the ion trap axis by superimposing a DC potential gradient on the trapping radio frequency potential. While Gerlich and coworkers used a collinear arrangement of the ion trap and TOF mass spectrometer, we describe an alternative approach here, in which the TOF spectrometer is mounted perpendicularly to the trap axis, allowing for direct optical access along the ion trap axis. Six independently adjustable DC voltages applied along the ion trap axis are used to focus the ion packet, overlap it with the photodissociation laser pulse and measure TOF mass spectra with high collection efficiency.

## INSTRUMENT DESIGN

A schematic of the 10K ring electrode trap – tandem mass spectrometer is shown in Figure 1. The spectrometer is housed in a vacuum chamber consisting of five differentially pumped stages. The molecular beam ion source used for the present experiments consists of 0.001” diameter sapphire nozzle, through which a gas mixture is expanded into the first stage of the vacuum chamber, labeled (a) in Figure 1. Ions are produced by crossing the continuous molecular beam with a 300.  $\mu$ A, 1 keV electron beam. Positively charged ions are formed by ionization and cooled in the supersonic expansion, promoting cluster forming reactions of the nascent ions. The ion beam is sampled by a 3 mm diameter skimmer and focused into the 22 cm long radio frequency (RF) linear decapole ion guide, labeled (b) in Figure 1. The RF ion guide, which is operated at 3.9 MHz and  $U_{\max} = \pm 400$  V can be filled with He buffer gas in order to collimate the ion beam and compress it in phase space. Ions of interest are mass selected in an Extrel CMS quadrupole mass tri-filter with a 2-2000 amu mass range, deflected into 90° by an electrostatic quadrupole ion deflector and focused into the linear RF ion trap.

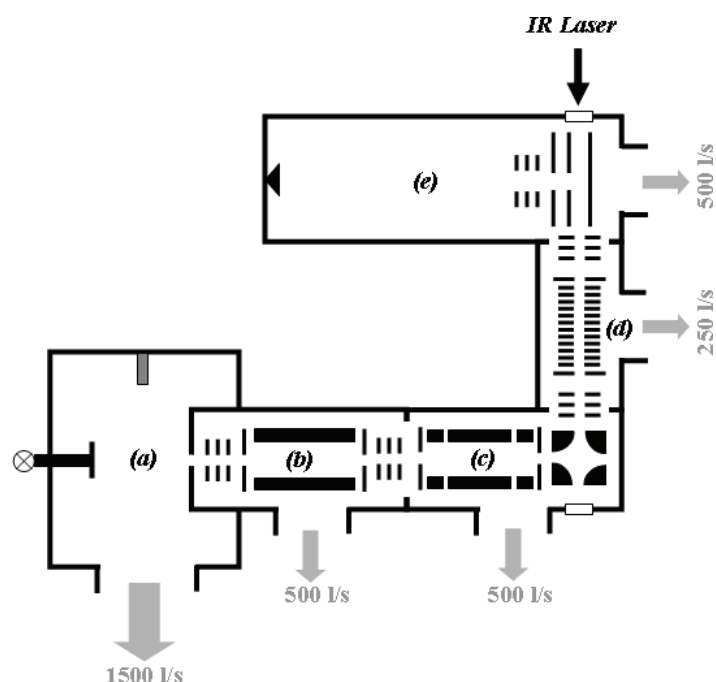


**FIGURE 1.** Schematic of the ion trap - tandem mass spectrometer: (a) Ion source, (b) RF linear ion guide, (c) quadrupole mass filter, (d) cryogenically cooled RF ring-electrode ion trap, and (e) linear TOF mass spectrometer. The vacuum chamber is differentially pumped by five turbo molecular pumps. The IR photodissociation laser is applied collinearly to the ion trap axis and timed such that it interacts with the ion packet at the center of the TOF mass spectrometer extraction region.

The RF ring electrode trap is based on the previous design of Gerlich and co-workers.<sup>16</sup> It consists of 24 concentric, 1 mm thick, Molybdenum ring electrodes with a 10 mm inner diameter. The electrodes are electrically isolated from one another by a set of interlocking 1 mm thick sapphire disks, making the entire assembly a gas-tight cylinder. Trapping requirements in the radial direction are met by application of an appropriate RF voltage (1.7 MHz,  $U_{\max} = \pm 350\text{V}$ ) with opposite phases applied to adjacent ring electrodes. Static DC potentials are applied to the entrance and exit lenses of the ion trap (electrodes A and B in Figure 2a), which confine the ion packet in the axial direction. A continuous flow of He buffer gas is introduced into the trap via a hole in one of the center electrodes and allows continuously filling, storing and thermalizing ions without switching any potentials.<sup>9</sup> Six individually adjustable, fast switching ( $\sim 2\mu\text{s}$  rise time) DC potentials, superimposed on the RF voltage, are applied to each set of four adjacent ring electrodes in order to control the field gradient along the trap axis (see Figure 2). This allows to control the position of the ion cloud inside the ion trap, as well as to quickly switch the trap DC voltages between two different configurations, i.e., the filling and the extracting cycles (see below). The trap is mounted to the cold head of a Sumitomo Heavy Industries closed cycle He cryostat. A heating cartridge installed in-between the cold head and the ion trap allows for a continuous temperature control over the range from approximately 10 to 350 K.

The DC voltages applied to the various electrodes during the three periods comprising a typical measurement cycle are schematically shown in Figure 2. First, the trap is loaded (Figure 2b). This is done by choosing appropriate voltages such that

the ion kinetic energy allows the ions to barely pass the potential barrier at the ion trap entrance. The ions then traverse the ion trap, are reflected at the exit lens and return to the entrance lens region. At this point the ions have lost sufficient kinetic energy through many collisions with the buffer gas, generally helium, such that they cannot pass the potential barrier at the entrance lens and are thus confined to the region within the ion trap. Further collisions with the buffer gas cools the ions both internally and also reduces the ion kinetic energy via momentum transfer so they remain in the trap.

Second, all ions are extracted from the trap using a tailored voltage ramp (see Figure 2c) and pass an Einzel lens. This arrangement allows focusing the ion cloud in space and time at the center of the extraction region of the orthogonally-mounted TOF mass spectrometer in order to optimize the ion detection efficiency. Third, the ions interact with the photodissociation laser pulse and a TOF mass spectrum is measured by applying high-voltage pulses to the extraction and acceleration plates (see Figure 2d).

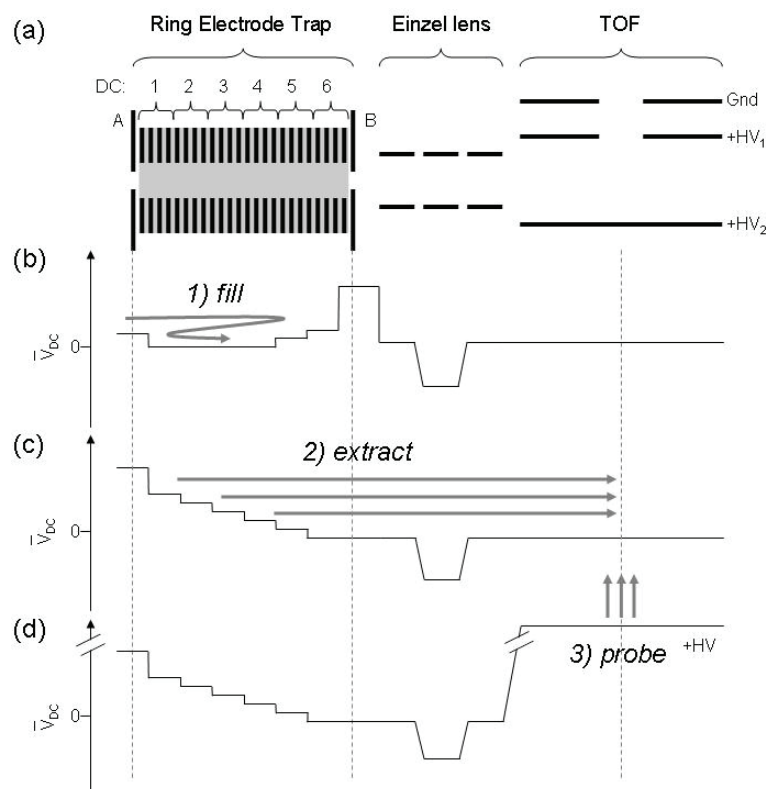


**FIGURE 2.** (a) Schematic of the ion trap – TOF mass spectrometer region. (b)-(d): Potential energy diagram indicating typical DC voltages applied to the electrodes shown in part (a) during the three periods comprising the measurement cycle. (b) The ion trap is continuously filled with mass-selected ions. (c) All ions are extracted from the ion trap into the extraction region of the TOF mass spectrometer. (d) The ions interact with the photodissociation laser pulse and a TOF mass spectrum is measured by applying high-voltage pulses to the extraction and acceleration plates.

The linear Wiley-McLaren<sup>17</sup> TOF mass spectrometer is mounted in an orthogonal arrangement to the trap axis, which allows direct laser access to ions along this axis. During the trap extraction, the TOF electrodes are held at ground potential. Two Behlke Power Electronics GmbH fast push-pull switches are used to produce short

high voltage pulses on the TOF electrodes ( $V_{\text{max}} = \pm 5000$  V,  $< 1$   $\mu\text{s}$  rise time) when the ions have reached the sampling region. The TOF extraction and acceleration plates have a 20 mm sample aperture to ensure that a large portion of the traversing ion packet is sampled. The ions fly through a 55 cm field free region where they separate in time depending on their mass-to-charge ratio before impinging on the MCP detector. Typical operating conditions give mass spectra with a resolution of  $m/\Delta m = 55$ .

Two ion detectors are mounted in the chamber. The first, a channeltron electron multiplier, is mounted along the ion trap axis, after the TOF electrodes, in an off-axis configuration for counting and recording mass selected ions from the quadrupole mass filter. The signal is sent through an amplifier discriminator which produces TTL pulses that are sent directly to the counter. TOF spectra are recorded using a dual microchannel plate (MCP) detector mounted in a chevron configuration. The transient signals from the MCP are first amplified by a fast pre-amplifier and then sent to a 300 MHz, 12-bit digitizer (Acquiris DP310) installed in the PC for real-time data collection. All electronics are computer controlled using a National Instruments PXI-1033 controller equipped with a 6602, 80MHz counter/timer card, a 6723 card with 32 programmable 13-bit analog output voltages and a 6733 card with 8 programmable 16-bit analog output voltages. The outputs are divided and sent through amplifier stages to power ion optics or to send control voltages and TTL pulses to critical equipment.

Tunable infrared radiation is provided by a Laservision optical parametric oscillator (OPO) – optical parametric amplifier (OPA) system. The system is pumped by the 1064 nm fundamental output from a pulsed Nd:YAG laser (Innolas, Spitlight 600) operating at 10 Hz with a 7 ns pulse width and average pulse power of 500 mJ. The incoming pulse is divided into two components, one which is frequency doubled to 532nm before arriving at an angle tuned OPO that produces tunable radiation from 712 to 880 nm. The remaining 1064 nm beam is sent through a delay stage before being recombined with the output of the OPO in the OPA stage, which is comprised of a set of 4 KTA crystals, where difference frequency mixing produces continuously tunable infrared radiation covering 1350 – 5000 nm (ca. 35 – 0.5 mJ). The laser wavelength is calibrated on rovibrational transitions in  $\text{CH}_4$ ,  $\text{NH}_3$  or  $\text{H}_2\text{O}$  measured using a photoacoustic cell. The laser bandwidth is  $2.2$   $\text{cm}^{-1}$ . The laser pulse enters the vacuum chamber through one of two  $\text{CaF}_2$  windows; one set is mounted along the trap axis to allow access through the ion trap, while the second set is mounted orthogonal to the trap axis-TOF region.

## INSTRUMENT OPERATION

A typical quadrupole mass spectrum obtained from ionization of a 0.1%  $\text{NH}_3$  in Ar gas mixture is shown in Figure 3.  $\text{NH}_x^+$  as well as  $\text{Ar}_{1-3}^+$  are the most abundantly formed ions under typical source conditions. Protonated ammonia clusters, like the protonated ammonia dimer  $\text{N}_2\text{H}_7^+$ , as well as the proton-bound complexes  $\text{NH}_{1-4}^+\cdot\text{Ar}$  are also formed. In the following we will use mass-selected  $\text{NH}_2^+\cdot\text{Ar}$  ions as an example for demonstrating, how IRPD spectra of buffer-gas cooled ions are measured using the present experimental setup.

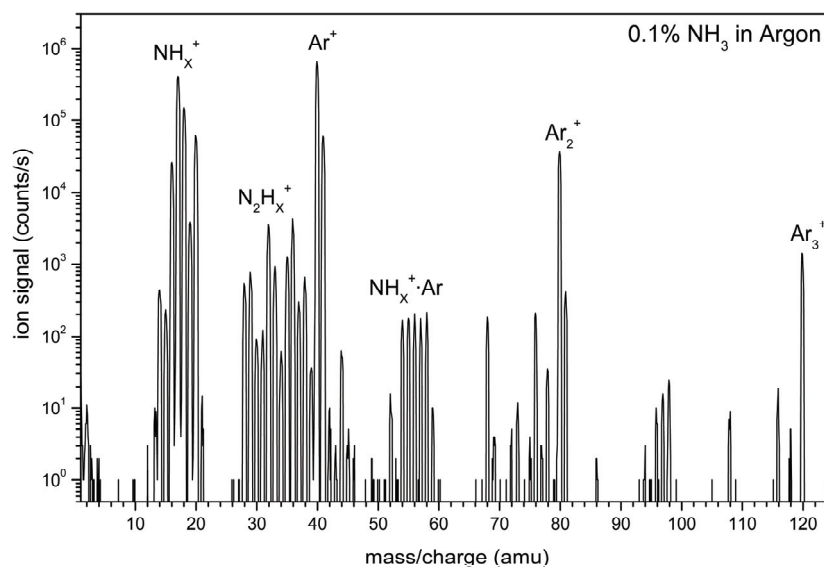


**FIGURE 3.** Quadrupole mass spectrum of the ions produced in the range from 2 to 125 amu by the electron impact ionization source.

Three characteristic TOF mass spectra are shown in Figure 4. They were measured by loading the ion trap ( $T_{\text{trap}} = 10$  K,  $p_{\text{trap}} \approx 10^{-2}$  mbar He) for 95 ms, extracting all ions from the ion trap into the extraction region of the orthogonally mounted TOF mass spectrometer, and then applying the high voltage pulses to the extraction plates after a fixed delay (70  $\mu\text{s}$ ).

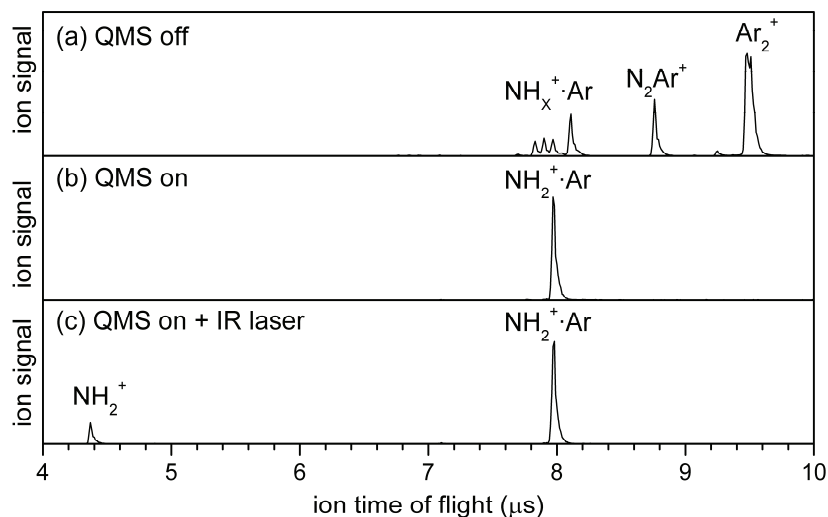


**FIGURE 4.** TOF mass spectra of trapped, buffer-gas cooled ions. (a) Quadrupole mass filter is off (RF only mode) and all ions are trapped. (b) Quadrupole mass filter is on and transmits only mass selected ions with  $\Delta m = 56$  amu. (c) Same as (b) but with the IR laser on resonance ( $3280$   $\text{cm}^{-1}$ ) with a vibrational transition in  $\text{NH}_2^+\cdot\text{Ar}$ , leading to the formation of  $\text{NH}_2^+$  photofragment ions.

In Figure 4a a TOF mass spectrum is shown with the quadrupole mass filter off. In this mode all ions are guided to the ion trap, trapped and then extracted. The observed ion distribution differs from the one shown in Figure 3, because the arrival time of the

ions in the extraction zone of the TOF mass spectrometer is mass dependent. For a given position inside the ion trap each ion is given the same kinetic energy upon extraction and consequently lighter ions arrive earlier and heavier ions later. In the present case, a delay time of 70  $\mu\text{s}$  between ion extraction from the ion trap and ion extraction into TOF mass spectrometer maximizes the  $\text{NH}_2^+\text{Ar}$  ion signal. Figure 4b shows a TOF mass spectrum measured with the quadrupole mass filter set to  $\Delta m=56$  amu. In this case only mass-selected ions are trapped, thermalized and reach the extraction region of the TOF mass spectrometer. Figure 4c shows a TOF spectrum measured under the same conditions as the previous spectra, but the ions are irradiated by an IR laser pulse before they are extracted into the TOF mass spectrometer. When resonant with a vibrational transition,  $\text{NH}_2^+\text{Ar}$  ions can absorb a photon. Because the photon energy is larger than the Ar binding energy in this case, intramolecular vibrational energy redistribution will lead to vibrational predissociation and production of  $\text{NH}_2^+$  photofragment ions.

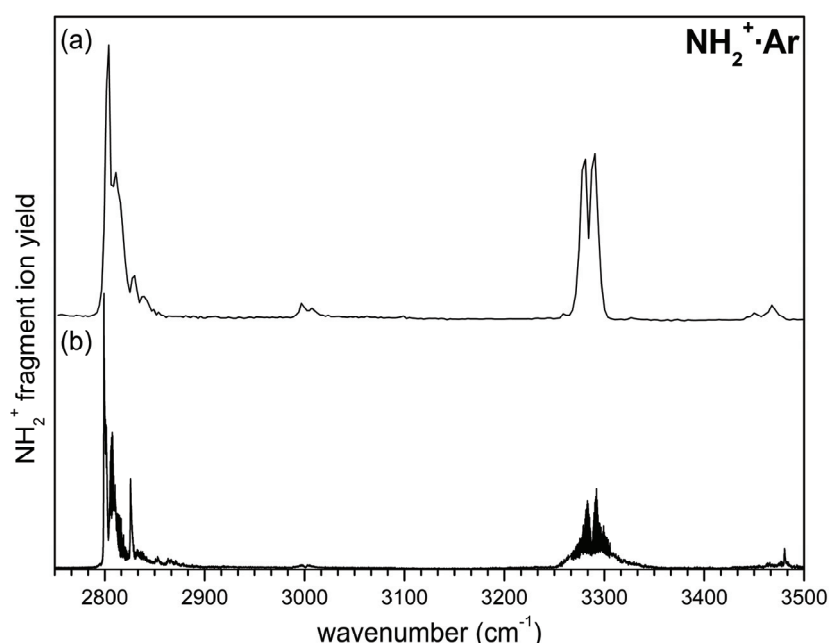


**FIGURE 5.** Infrared photodissociation spectra of  $\text{NH}_2^+\text{Ar}$ . (a) IRPD spectrum obtained with the present experimental setup. (b) IRPD spectra obtained by Nizkorodov et al.<sup>18</sup>

An IRPD spectrum is measured by monitoring the fragment ion yield as a function of the irradiation wavelength. The IRPD spectrum of trapped, buffer-gas cooled  $\text{NH}_2^+\text{Ar}$  ions, measured by monitoring the  $\text{NH}_2^+$  fragment ion intensity, is shown in Figure 5, along with the previously recorded high resolution spectrum by Nizkorodov et al.<sup>18</sup> The two spectra are in good agreement, indicating that the present instrument yields reliable IRPD spectra. Band assignments can be found elsewhere<sup>18-20</sup>. Differences between the two spectra are mainly due to the different bandwidths of the IR lasers used and, to a lesser extent, due to differences in ion temperature. The previous high resolution data is composed of a number of scans over smaller wavelength ranges which were then combined, while our spectrum was recorded in a single scan.

## CONCLUSIONS

A novel instrumental setup for measuring IRPD spectra of buffer gas cooled, mass-selected ions has been described and successfully tested. It combines a cryogenically cooled, linear RF ion trap with a tandem mass spectrometer, optimally coupling continuous ion sources to pulsed laser experiments. The use of independently adjustable DC potentials superimposed with the trapping radio frequency field provides control over the ion distribution within, as well as the kinetic energy distribution of the ions extracted from the ion trap. Future improvements will include the addition of a reflectron stage for improved mass resolution, while a fast switch to rapidly turn off the RF field during ion extraction may further improve the collection efficiency in the TOF mass spectrometer region. Addition of extra DC potentials, one for each ring electrode, would provide increased control of the trap operation. Finally, a multipass arrangement is currently being designed to allow each laser pulse to interact with the ions several times, which will increase the photofragment ion yield.

## ACKNOWLEDGMENTS

KRA thanks Dieter Gerlich for help in the design of the ring electrode ion trap and for many fruitful discussions.

## REFERENCES

1. M. Maier-Borst, D.B. Cameron, M. Rokni, and J.H. Parks, *Phys. Rev. A* **59**, R3162-R3165 (1999).
2. A. Lechtken, D. Schooss, J.R. Stairs, M.N. Blom, F. Furche, N. Morgner, O. Kostko, B. von Issendorff, and M.M. Kappes, *Angew. Chem. Int. Ed.* **46**, 2944-2948 (2007).
3. M. T. Bowers, P. R. Kemper, G. Von Helden, and P. A. M. Van Koppen, *Science* **260**, 1446-1451 (1993).
4. P. Dugourd, R.R. Hudgins, D.E. Clemmer, and M.F. Jarrold, *Rev. Sci. Instrum.* **68**, 1122-1129 (1997).
5. M.A. Duncan, *Int. J. Mass Spectrom.* **200**, 545-569 (2000).
6. E.J. Bieske and O. Dopfer, *Chem. Rev.* **100**, 3963-3998 (2000).
7. J. Oomens, B.G. Sartakov, G. Meijer, and G. von Helden, *Int. J. Mass Spectrom.* **254**, 1-19 (2006).
8. K. R. Asmis, A. Fielicke, G. von Helden, and G. Meijer, in *The Chemical Physics of Solid Surfaces. Atomic Clusters: From Gas Phase to Deposited*, edited by D.P. Woodruff (Elsevier, Amsterdam, 2007), Vol. 12, pp. 327-375.
9. G. G. Dolnikowski, M. J. Kristo, C. G. Enke, and J. T. Watson, *Int. J. Mass Spectrom.* **82**, 1-15 (1988).
10. D. Gerlich, *Adv. Chem. Phys.* **82**, 1 (1992).
11. T. Leisner, S. Vajda, S. Wolf, L. Wöste, and R.S. Berry, *J. Chem. Phys.* **111**, 1017 (1999).
12. K.R. Asmis, M. Brümmer, C. Kaposta, G. Santambrogio, G. von Helden, G. Meijer, K. Rademann, and L. Wöste, *Phys. Chem. Chem. Phys.* **4**, 1101-1104 (2002).
13. Y. S. Wang, C. H. Tsai, Y. T. Lee, H. C. Chang, J. C. Jiang, O. Asvany, S. Schlemmer, and D. Gerlich, *J. Phys. Chem. A* **107**, 4217-4225 (2003).
14. O. V. Boyarkin, S. R. Mercier, A. Kamariotis, and T. R. Rizzo, *J. Am. Chem. Soc.* **128**, 2816-2817 (2006).
15. J. Glosik, P. Hlavenka, R. Plasil, F. Windisch, D. Gerlich, A. Wolf, and H. Kreckel, *Philos. Trans. R. Soc. London, Ser. A* **364**, 2931-2942 (2006).
16. A. Luca, S. Schlemmer, I. Cermak, and D. Gerlich, *Rev. Sci. Instrum.* **72**, 2900-2908 (2001).
17. W. C. Wiley and I. H. McLaren, *Rev. Sci. Instrum.* **26**, 1150-1157 (1955).
18. S. A. Nizkorodov, M. Meuwly, J. P. Maier, O. Dopfer, and E. J. Bieske, *J. Chem. Phys.* **108**, 8964-8975 (1998).
19. O. Dopfer, N. Solca, R. V. Olkhov, and J. P. Maier, *Chem. Phys.* **283**, 85-110 (2002).
20. N. M. Lakin, R. V. Olkhov, and O. Dopfer, *Faraday Discuss.* **118**, 455-476 (2001).